FOREX Publication
Open Access | Rapid and quality publishing
International Journal of
Electrical and Electronics Research (IJEER)
Research Article | Volume 12, Issue 2 | Pages 520-528 | e-ISSN: 2347-470X

Control for Wind Turbine System using PMSG when Wind Speed Changes

Pham Van Minh

Faculty of Electrical-Automation, University of Economics-Technology for Industries, Hanoi, Vietnam; pvminh@uneti.edu.vn

***Correspondence:** Pham Van Minh; pvminh@uneti.edu.vn

ABSTRACT- This paper presents the proposed model to control grid-connected wind turbine by permanent magnet synchronous generator (PMSG). With the wind speed changing continuously, the rotor system needs to be able to self-regulate according to wind speed and direction to ensure efficient operation of the turbine. The PMSG was chosen because the magnetic flux is always available thanks to the permanent magnet system glued to the rotor surface. The generator provides power with low rotational speed but high efficiency. These are the important advantages of using PMSG for wind turbine. MATLAB - Simulink software was used to design the controllers and the survey results proved that this control system meets the power quality requirements when connecting to the grid and optimizing the energy conversion process for turbine wind.

Keywords: wind energy conversion system, permanent magnet synchronous generator, maximum power point tracking, generator side converter, wind turbine.

ARTICLE INFORMATION

Author(s): Pham Van Minh;

Received: 19/02/2024; **Accepted**: 11/04/2024; **Published**: 30/05/2024;
e-ISSN: 2347-470X;
Paper Id: IJEER 1902-13;
Citation: 10.37391/IJEER.120225
Webpage-link:
https://ijeer.forexjournal.co.in/archive/volume-12/ijeer-120225.html

crossref member
CROSSREF.ORG THE CITATION LINKING BACKBONE

Publisher's Note: FOREX Publication stays neutral with regard to Jurisdictional claims in Published maps and institutional affiliations.

1. INTRODUCTION

Wind energy conversion system (WECS) is a renewable energy source that is harnessed from wind power. It has been used for thousands of years to power humans. Currently, wind turbine technology has developed rapidly and has become a popular method for generating electricity from wind energy.

PMSG is one of the remarkable technologies in this field [1-5]. These generators are constructed with a permanent magnet rotor, ie the magnet is capable of generating a constant amount of magnetism. This helps to increase efficiency and reduce energy loss during the energy conversion from wind to electricity. PMSGs work well at low revs, are flexibly adjusted and self-adjust according to wind speed and direction. This optimizes the intake of energy from the wind and automatically adjusts the wind turbine's rotational speed for optimal operation [6-8].

Wind energy from PMSGs has many advantages. It is a clean energy source, causing no fuel emissions or environmental pollution [9-11]. Wind energy is also an unlimited source of renewable energy, because wind power has always existed on our planet. This helps to ensure a stable and sustainable energy supply in the future. With the development and advancement of technology, wind energy is becoming more and more an important way to meet energy demand and reduce environmental pollution. The use of PMSGs in generating electricity from wind energy contributes to the construction of a clean and sustainable energy system for the future [12-14].

Wind turbines need to have the highest efficiency to improve the quality of wind energy obtained. In which, improving the control mechanism of the wind energy system plays an important role. Above rated wind speed, modern wind energy systems often apply the Maximum Power Point Tracking (MPPT) mechanism based on the best characteristic curve. This mechanism is capable of adjusting the mechanical output of the generator to match the requirements of the wind turbine in different weather conditions [15-18].

In addition, wind speed, blade direction and rotor rotation speed are also important factors affecting the wind energy capture of turbines. The random variation of the wind source and the energy loss in the WECS also affects the stability of the system. Therefore, the conversion of wind energy to electricity is not a simple linear process, but often encounters considerable volatility and uncertainty. In recent studies and literature, many theories and control strategies have been proposed to solve the problems of PMSGs in wind energy systems. The main objective of the control strategies is to maximize the capacity utilization efficiency and to adjust the desired power factor and reactive power required by the grid. These tasks are performed simultaneously using the appropriate line voltage. The global model of a PMSG based on a wind energy system is detailed in the research papers [19, 20].

Although the PID algorithm is highly reliable and easy to implement, when the system works in extreme weather conditions, with wind speed and model parameters changing, this controller is no longer suitable [21, 22]. Therefore, a number of nonlinear control schemes have been developed and applied in wind turbine systems to improve power quality. One of these methods is fuzzy control, which uses discontinuous control rules to build models [23-25]. However, the use of these discontinuous control laws can cause noise, affect control accuracy, and lead to significant heat loss in electrical circuits as well as increased wear of the components moving mechanical parts. To overcome the disadvantages of the SMC method [26-28], a number of other methods have been studied and applied in PMSG wind turbine systems. For example, optimized control based on Scalar Algorithm has been proposed to optimize PMSG wind turbine performance under different conditions [29-31]. This method uses an optimization algorithm to adjust the parameters of the PMSG wind turbine, in order to achieve maximum efficiency and reduce energy loss.

In addition, intelligent control approaches such as reinforcement learning (RL) have been applied to improve the efficiency of the PMSG wind turbine system [32-35]. The RL method uses machine learning algorithms to find optimal control policies and improve performance over time. This helps the PMSG wind turbine system automatically adapt to environmental conditions and optimize power efficiency. In addition, the control method using artificial neural network (ANN) has also been applied in the WECS using PMSG [36-39].

Although there are many limitations and challenges in applying nonlinear control methods to PMSG wind turbine systems, further research is conducted to bring about significant improvements in the efficiency and reliability of the wind turbines system.

2. SYSTEM MODELLING

WECS using a PMSG (PMSG) consists of components as shown in *figure 1*.

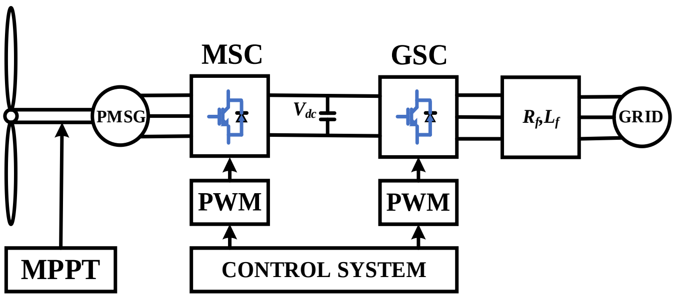

Figure 1. Components of a WECS

Wind turbine: The main moving component that collects wind energy. Wind turbines usually consist of a propeller and a rotating shaft, designed to take advantage of the thrust from the wind and convert it into mechanical energy.

PMSG Generator: This is a PMSG, which is fixed on the axis of rotation of the wind turbine. The PMSG generator consists of a permanent magnet rotor and a coiled stator. As the wind turbine rotates, the rotor also rotates creating alternating current in the windings of the stator, generating electricity.

System control: The control system will manage and regulate the operation of the WECS. It will monitor parameters such as wind speed, velocity and position of the wind turbine, and information from the PMSG transmitter to adjust the speed and power of the wind turbine, ensuring the highest and stable performance.

Inverter: The inverter is used to convert the alternating current from the PMSG generator into alternating current that is suitable for the frequency and voltage of the power grid. This inverter will adjust the output frequency and voltage to synchronize with the power grid and supply power.

Grid: The output of the inverter will be connected to the grid through a system that connects and converts parameters such as voltage, frequency and power. The WECS using PMSG generator will supply electricity synchronously to the grid, meeting the demand for electricity.

Thereby, the WECS using PMSG generator helps to convert wind energy into electronic electricity and supply it to the grid, playing an important role in the utilization and development of renewable energy from electricity wind.

2.1 Wind Turbine Modelling

The mathematical model of a wind turbine is based on kinetic and energy principles. This model helps to simulate and predict the operation of wind turbines under different conditions.

The mechanical energy $\mathcal{E}$ of a mass of air m moving with velocity υ is:

$$\mathcal{E} = \frac{1}{2}m\upsilon^2 \tag{1}$$

The power $\mathcal{P}$ obtained depends on the mass of the moving air, the wind speed, the air density ρ, the cross-section $\mathcal{S}$ of the propeller rotation.

$$\mathcal{P}_{win} = \frac{1}{2}\rho\mathcal{S}\upsilon^3 \tag{2}$$

According to [2-6], the power of wind turbine is calculated by the expression:

$$\mathcal{P}_{tur} = \mathcal{C}_p(\lambda,\beta) \times \mathcal{P}_{win} = \frac{1}{2}\mathcal{C}_p(\lambda,\beta)\rho\mathcal{S}\upsilon^3 \tag{3}$$

In there:

$\mathcal{P}_{tur}$: Turbine output power (W); $\mathcal{C}_p(\lambda,\beta)$: Energy conversion coefficient (is the ratio between blade tip speed λ and blade angle β); $\mathcal{S}$: Rotating cross-section of the propeller (m^2); ρ: Density of the air (kg/m^3); υ speed of the wind (m/s). From formula (3), we see that wind speed is the most important factor of power, when wind speed increases once, the output power also increases by a power of three.

The energy conversion coefficient $\mathcal{C}_p(\lambda,\beta)$ of formula (3) according to [2-6], is calculated as follows:

$$\mathcal{C}_p(\lambda,\beta) = 0.5176\left(\frac{116}{\lambda_1} - 0.4\beta - 5\right)e^{\frac{-21}{\lambda_1}} + 0.0068\lambda \Rightarrow \frac{1}{\lambda_1} = \frac{1}{\lambda+0.08\beta} - \frac{0.035}{1+\beta^3} \quad (4)$$

The ratio of wind turbine blade tip speed to wind speed is:

$$\lambda = \frac{\mathcal{R}\omega_{tur}}{\upsilon} \quad (5)$$

where ω_{tur} is the rotational speed of the turbine which is also the rotor angular velocity, R radius of the turbine.

From *equation (3)* we have:

$$\mathcal{P}_{tur} = \frac{1}{2}\mathcal{C}_p(\lambda,\beta)\rho\pi\mathcal{R}^2\upsilon^3 \quad (6)$$

According to [1-5], the wind turbine torque is calculated as follows:

$$\mathcal{T}_{tur} = \frac{\mathcal{P}_{tur}}{\omega_{tur}} = \frac{1}{2\lambda^3}\mathcal{C}_p(\lambda,\beta)\rho\pi\mathcal{R}^5\omega_{tur}^2 \quad (7)$$

2.2 PMSG Modeling

Through the use of physical principles and formulas, mathematical modeling can help predict and simulate the motion and performance of PMSGs under various conditions. However, in order to build a detailed and accurate model, the specific specifications of the PMSG are required [1-6].

The stator voltage (also known as open-circuit voltage) of a PMSG is the voltage measured at the output of the generator when no connected load is connected. This is the voltage that a synchronous generator can supply when operating in an uncertain state and without securing the application load motor. The voltage stator of a PMSG can be tailored to suit the specific requirements of the application. In common industrial applications, the stator voltage is usually defined in the generator specifications. Normally, the stator voltage of a PMSG will be higher than the rated voltage of the generator, which helps to ensure that the generator is capable of providing sufficient voltage for the load connections in the electrical network. The stator voltage is represented by the equation [2-5].

The equivalent circuit of the PMSG in the d-q rotary reference system can be shown in *figure 2*.

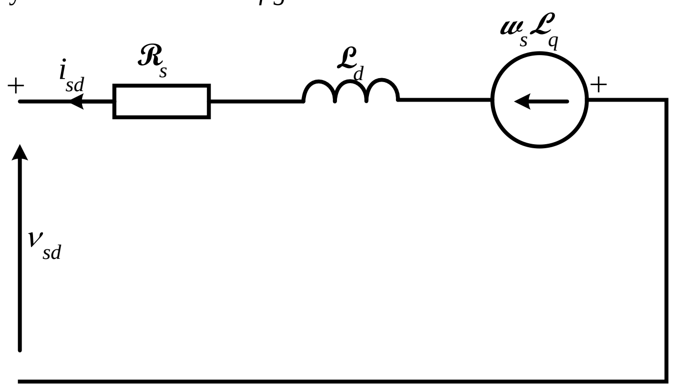

(a)

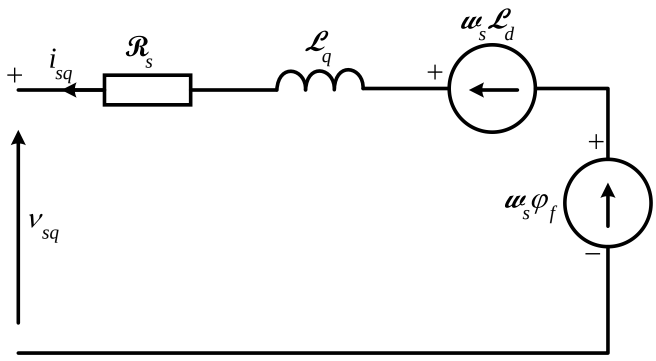

(b)

Figure 2. Equivalent diagram of generator PMSG

$$\begin{cases} \mathcal{V}_{sd} = \mathcal{R}_s i_{sd} + \frac{d\phi_d}{dt} - w_s\phi_q \\ \mathcal{V}_{sq} = \mathcal{R}_s i_{sq} + \frac{d\phi_q}{dt} + w_s\phi_d \end{cases} \quad (8)$$

Calculation of stator flux of a PMSG is done through the following equation:

$$\begin{cases} \phi_q = \mathcal{L}_q i_{sq} \\ \phi_d = \mathcal{L}_d i_{sd} + \varphi_f \end{cases} \quad (9)$$

Replacing the expression of equation (9) with the corresponding variables in equation (8) will get:

$$\begin{cases} \mathcal{V}_{sd} = \mathcal{R}_s i_{sd} + \mathcal{L}_d\frac{di_{sd}}{dt} - w_s\mathcal{L}_q i_{sq} \\ \mathcal{V}_{sq} = \mathcal{R}_s i_{sq} + \mathcal{L}_q\frac{di_{sq}}{dt} + w_s\mathcal{L}_d i_{sd} + w_s\varphi_f \end{cases} \quad (10)$$

In the Park system, the PMSG machine electromagnetic module expression can be represented as follows:

$$\begin{cases} \mathcal{T}_{tur} - \mathcal{T}_{em} = \mathcal{J}\frac{d\omega}{dt} + f_c\omega \\ \mathcal{T}_{em} = 1.5p\left[(\mathcal{L}_d - \mathcal{L}_q)i_{sd}i_{sq} + i_{sq}\varphi_f\right] \end{cases} \quad (11)$$

The following equations are used to calculate active and reactive power in WECS using PMSG, based on voltage and current flowing through the circuit:

$$\begin{cases} \mathcal{P}_{gen} = 1.5(\mathcal{V}_{sd}i_{sd} + \mathcal{V}_{sq}i_{sq}) \\ \mathcal{Q}_{gen} = 1.5(\mathcal{V}_{sq}i_{sd} + \mathcal{V}_{sd}i_{sq}) \end{cases} \quad (12)$$

2.3 Generator Side Converter Model

The input voltage from the WECS is decomposed into two components: a component from the d axis $\mathcal{V}_{sd}$ and a component from the q axis $\mathcal{V}_{sq}$. The current is represented by i_{sd} and i_{sq}, and the relationship between i_{sd} and i_{sq} and $\mathcal{V}_{sd}$ and $\mathcal{V}_{sq}$ can be described by *equation (10)*. This allows the solenoid current to be adjusted according to the input voltage. The mechanical speed of the rotor and the motor power input from the generator through the rotor are calculated using the equations above. This allows the generator output power to be adjusted.

International Journal of
Electrical and Electronics Research (IJEER)
Research Article | Volume 12, Issue 2 | Pages 520-528 | e-ISSN: 2347-470X

By adjusting the stator voltage of the generator, it is possible to adjust the mechanical current and speed, thereby adjusting the output power of the PMSG generator. This is the basic modeling for the generator-side converter of a PMSG generator, and it allows for tuning and monitoring of the generator output performance based on control variables such as voltage. From *equations (10), (11)* and $\omega_s = p\omega$ the generator-side converter is rewritten as:

$$\begin{cases} \frac{di_{sd}}{dt} = \frac{1}{L_d}\left(-R_s i_{sd} + p\omega L_q i_{sq} + V_{sd}\right) \\ \frac{di_{sq}}{dt} = \frac{1}{L_q}\left(-R_s i_{sq} - p\omega L_d i_{sd} - p\omega\varphi_f + V_{sq}\right) \\ \frac{d\omega}{dt} = \frac{1}{J}\left(T_{tur} - T_{em} - f_c\omega\right) \end{cases} \quad (13)$$

The key to achieving maximum electromechanical torque operation is to set the stator current to zero. We can then choose the reference current ($i_{sd-ref} = 0$), which means the actual d axis current (i_{sd}) is adjusted to match the reference value is zero. The contribution of the magnetization field is regulated only by the current on the q axis (i_{sq}), allowing the final output voltage to be generated. By eliminating the current component in the stator, we maximize the output power by increasing the electromechanical torque generated by the machine. This configuration helps to optimize the performance of PMSG.

$$\begin{cases} V_{sd} = -p\omega L_q i_{sq} \\ \frac{di_{sq}}{dt} = \frac{1}{L_q}\left(-R_s i_{sq} - p\omega\varphi_f + V_{sq}\right) \end{cases} \quad (14)$$

By taking the steps of current regulation as described, we can maximize the electromagnetic torque of the generator:

$$T_{em\_opt} = 1.5 p i_{sq}\varphi_f \quad (15)$$

Where L_d and L_q: generator inductance on axes d and q (H); R_s: stator resistance (Ω); i_{sd} and i_{sq}: current on axes d and q (A); V_{sd} and V_{sq}: voltages on the d and q axes (V); ω: rotor angular velocity (rad/s); φ_f: magnetic flux of the permanent magnet (Wb); p: number of pole pairs.

3. CONTROLLER DESIGN

3.1 MPPT Control

The controller used to optimize generator output efficiency is called MPPT. An important point in MPPT is the electromagnetic torque regulation of the generator. Input voltage and current parameters are measured and used to calculate current electromagnetic torque. By comparing the current electromagnetic torque with the maximum applicable electromagnetic torque, the required rotational speed adjustment direction for the generator can be determined. By keeping the wind turbine at this speed rotary, we can achieve optimized power output under different wind conditions and ensure efficient operation of the generator.

$$T_{tur\_ref} = \frac{P_{tur\_ref}}{\omega_{tur}} = \frac{1}{2\lambda_{opt}^3} C_p\left(\lambda_{opt}\right)\rho\pi R^5\omega_{tur}^2 \quad (16)$$

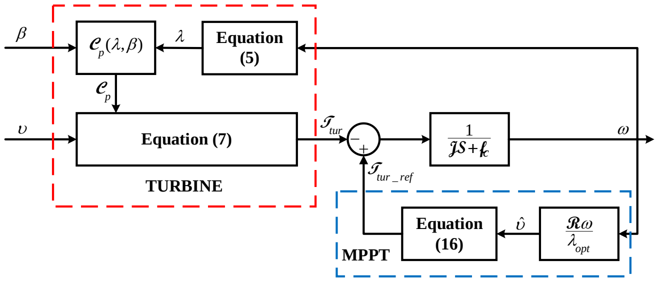

Figure 3. Wind turbine control diagram and MPPT

When the wind speed changes, the control angle adjusts the tilt angle of the blades to ensure the wind generator operates at a preset point (unlimited to the optimal mode) and avoids operation in any abnormal area. okay or not safe.

When the wind speed is too weak, the tilt angle of the blades will be adjusted to increase the efficiency of energy recovery from the wind. Conversely, when the wind speed increases to a certain extent, the tilt angle of the blades will be adjusted to reduce drag and prevent the wind generator from overloading. The tilt angle control technique is an important part of the wind generator system, and it is accomplished through the use of wind speed sensors and control information to adjust the engine and the tilt angle of the wind generator. fan blades. This tilt angle adjustment helps to ensure that the wind generator operates at its optimum point, increasing efficiency and at the same time protecting the generator from overload and unsafe operation.

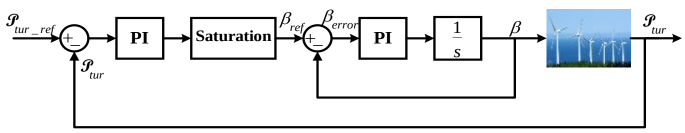

Figure 4. Wind turbine blade tilt angle control diagram

3.2 GSC control using backstepping

The way backstepping works is to use continuous and incremental control steps to achieve the control goal. Stepping control begins by establishing a mathematical model of the wind turbine system, then defining control steps and objectives to optimize performance or ensure operational safety.

Subsequent control steps are calculated using the driver's control methods and starting parameters such as actual wind speed, drag, and lift. Furthermore, the control steps can also be adjusted to accommodate variable factors such as variable wind speed.

Backstepping technology allows more flexible and precise operation control in wind turbine systems. It helps to optimize performance and save power, while ensuring safe and stable operation of the system.

The applied strategy is then separated into two consecutive phases. In the first stage, the necessary instructions are provided

FOREX Publication
Open Access | Rapid and quality publishing

International Journal of
Electrical and Electronics Research (IJEER)
Research Article | Volume 12, Issue 2 | Pages 520-528 | e-ISSN: 2347-470X

for the second stage. Specifically, the state and control vectors are selected as follows:

State vector $[x] = [x_1\ x_2\ x_3]^T = [i_{sd}\ i_{sq}\ \omega]^T$

Control vector $[u] = [\mathcal{V}_{sd}\ \mathcal{V}_{sq}]^T$

The first phase of the strategy focuses on defining the guidelines and parameters needed for the next phase. Specifically, the x state stack is defined using the x_1, x_2 and x_3 variables i_{sd}, $i_{sq}$and ω, respectively, and the scene control u is defined using the variables $\mathcal{V}_{sd}$ and $\mathcal{V}_{sq}$.

These instructions and parameters will be used in the second phase of the strategy, with the goal of tuning and directing the control system to the defined control and status displays.

Definition of speed tracking error:

$$e_\omega = \omega - \omega_{ref} \tag{17}$$

Derivative of both sides of *equation (17):*

$$\dot{e}_\omega = \dot{\omega}_{ref} - \dot{\omega} = \dot{\omega}_{ref} - \frac{1}{\mathcal{J}}(\mathcal{T}_{tur} - \mathcal{T}_{em} - f_c\omega)$$
$$= \dot{\omega}_{ref} - \frac{1}{\mathcal{J}}\{\mathcal{T}_{tur} - 1.5\wp[(\mathcal{L}_d - \mathcal{L}_q)i_{sd}i_{sq} + i_{sq}\varphi_f] - f_c\omega\} \tag{18}$$

Choose a Lyapunov function of the following form:

$$\mathbb{V}_1 = \frac{1}{2}e_\omega^2 \tag{19}$$

First derivative of $\mathbb{V}_1$ with respect to time:

$$\dot{\mathbb{V}}_1 = e_\omega\dot{e}_\omega = -\mathbb{K}_\omega e_\omega^2 + \frac{e_\omega}{\mathcal{J}}(f_c\omega - \mathcal{T}_{tur} + \mathbb{K}_\omega \mathcal{J} e_\omega + 1.5\wp i_{sq}\varphi_f)$$
$$+ \frac{1.5}{\mathcal{J}}\wp(\mathcal{L}_d - \mathcal{L}_q)i_{sd}i_{sq}e_\omega \tag{20}$$

Where $\mathbb{K}_\omega$ is a positive constant; select the stator current values isd and isq so that $\dot{\mathbb{V}}_1$ is negative.

$$\dot{\mathbb{V}}_1 = -\mathbb{K}_\omega e_\omega^2 \leq 0 \tag{21}$$

So system (13) is stable.

Next define the stator current errors:

$$\begin{cases} e_{sd} = i_{sd\_ref} - i_{sd} \\ e_{sq} = i_{sq\_ref} - i_{sq} \end{cases} \tag{22}$$

Derivative of both sides of equation (22):

$$\begin{cases} \dot{e}_{sd} = \overset{*}{i}_{sd\_ref} - \overset{*}{i}_{sd} \\ \dot{e}_{sq} = \overset{*}{i}_{sq\_ref} - \overset{*}{i}_{sq} \end{cases} \tag{23}$$

$$\dot{e}_{sd} = \overset{*}{i}_{sd\_ref} - \overset{*}{i}_{sd} = 0 - \overset{*}{i}_{sd} = -\frac{di_{sd}}{dt} = \frac{1}{\mathcal{L}_d}(\mathcal{R}_s i_{sd} - \wp\omega\mathcal{L}_q i_{sq} - \mathcal{V}_{sd}) \tag{24}$$

$$\dot{e}_{sq} = \overset{*}{i}_{sq_ref} - \overset{*}{i}_{sq} = \frac{2}{3\wp\varphi_f}(-f_c\dot{\omega} - \mathbb{K}_\omega\mathcal{J}\dot{e}_\omega) + \frac{1}{\mathcal{L}_q}(\mathcal{R}_s i_{sq} + \wp\omega\mathcal{L}_d i_{sd} + \wp\omega\varphi_f - \mathcal{V}_{sq}) = \frac{2}{3\wp\varphi_f}\Big\{-f_c\frac{1}{\mathcal{J}}(\mathcal{T}_{tur} - \mathcal{T}_{em} - f_c\omega) - \mathbb{K}_\omega\mathcal{J}\frac{1}{\mathcal{J}}\Big[-\mathcal{T}_{tur} + f_c\omega + \frac{3\wp}{2}\Big((\mathcal{L}_d - \mathcal{L}_q)i_{sd}i_{sq} + i_{sq}\varphi_f\Big)\Big]\Big\} + \frac{1}{\mathcal{L}_q}(\mathcal{R}_s i_{sq} + \wp\omega\mathcal{L}_d i_{sd} + \wp\omega\varphi_f - \mathcal{V}_{sq}) = \frac{2}{3\wp\mathcal{J}\varphi_f}\Big\{-f_c\Big[\mathcal{T}_{tur} - \frac{3\wp}{2}\Big((\mathcal{L}_d - \mathcal{L}_q)i_{sd}i_{sq} + i_{sq}\varphi_f\Big) - f_c\omega\Big] + \mathbb{K}_\omega\mathcal{J}\Big[\mathcal{T}_{tur} - f_c\omega - \frac{3\wp}{2}\Big((\mathcal{L}_d - \mathcal{L}_q)i_{sd}i_{sq} + i_{sq}\varphi_f\Big)\Big]\Big\} + \frac{1}{\mathcal{L}_q}(\mathcal{R}_s i_{sq} + \wp\omega\mathcal{L}_d i_{sd} + \wp\omega\varphi_f - \mathcal{V}_{sq}) = \frac{2}{3\wp\mathcal{J}\varphi_f}\Big\{(\mathbb{K}_\omega\mathcal{J} - f_c)\Big[\mathcal{T}_{tur} - f_c\omega - \frac{3\wp}{2}\Big((\mathcal{L}_d - \mathcal{L}_q)i_{sd}i_{sq} + i_{sq}\varphi_f\Big)\Big]\Big\} + \frac{1}{\mathcal{L}_q}(\mathcal{R}_s i_{sq} + \wp\omega\mathcal{L}_d i_{sd} + \wp\omega\varphi_f - \mathcal{V}_{sq}) \tag{25}$$

Choose the second Lyapunov function of the following form:

$$\mathbb{V}_2 = \frac{1}{2}(e_\omega^2 + e_{sd}^2 + e_{sq}^2) \tag{26}$$

Derivative of equation (26) with respect to time:

$$\dot{\mathbb{V}}_2 = e_\omega\dot{e}_\omega + e_{sd}\dot{e}_{sd} + e_{sq}\dot{e}_{sq} \tag{27}$$

$$\dot{\mathbb{V}}_2 = -\mathbb{K}_\omega e_\omega^2 - \mathbb{K}_{sd}e_{sd}^2 - \mathbb{K}_{sq}e_{sq}^2 + \frac{e_\omega}{\mathcal{J}}\Big[-\frac{3\wp}{2}\varphi_f e_{sq} - \frac{3\wp}{2}(\mathcal{L}_d - \mathcal{L}_q)i_{sq}e_{sq}\Big] + \frac{e_{sd}}{\mathcal{L}_d}(\mathcal{R}_s i_{sq} - \wp\omega\mathcal{L}_q i_{sq} - \mathcal{V}_{sd} + \mathbb{K}_{sd}\mathcal{L}_d e_{sd}) + \frac{e_{sq}}{\mathcal{L}_q}\Big\{\frac{2\mathcal{L}_q}{3\wp\mathcal{J}\varphi_f}\Big((\mathbb{K}_\omega\mathcal{J} - f_c)\Big[\mathcal{T}_{tur} - f_c\omega - \frac{3\wp}{2}\Big((\mathcal{L}_d - \mathcal{L}_q)i_{sd}i_{sq} + i_{sq}\varphi_f\Big)\Big]\Big)\mathcal{R}_s i_{sq} + \wp\omega\mathcal{L}_d i_{sd} + \wp\omega\varphi_f - \mathcal{V}_{sq} + \mathbb{K}_{sq}\mathcal{L}_q e_{sq}\Big\} \tag{28}$$

For a stable system, or negative $\dot{\mathbb{V}}_2$, the stator voltage is calculated:

$$\mathcal{V}_{sd\_ref} = \mathcal{R}_s i_{sd} - \wp\omega\mathcal{L}_q i_{sq} + \mathbb{K}_{sd}\mathcal{L}_d e_{sd} - \frac{3\wp}{2\mathcal{J}}\mathcal{L}_d(\mathcal{L}_d - \mathcal{L}_q)i_{sq}e_\omega \tag{29}$$

$$\mathcal{V}_{sq\_ref} = \frac{2\mathcal{L}_q}{3\wp\mathcal{J}\varphi_f}\Big((\mathbb{K}_\omega\mathcal{J} - f_c)\Big[\mathcal{T}_{tur} - f_c\omega - \frac{3\wp}{2}\Big((\mathcal{L}_d - \mathcal{L}_q)i_{sd}i_{sq} + i_{sq}\varphi_f\Big)\Big]\Big) + \mathcal{R}_s i_{sq} + \wp\omega\mathcal{L}_d i_{sd} + \wp\omega\varphi_f + \mathbb{K}_{sq}\mathcal{L}_q e_{sq} - \frac{3\wp}{2\mathcal{J}}\mathcal{L}_q\varphi_f e_\omega \tag{30}$$

The block diagram of the control system in WECS is shown in *figure 5.*

International Journal of
Electrical and Electronics Research (IJEER)
Research Article | Volume 12, Issue 2 | Pages 520-528 | e-ISSN: 2347-470X

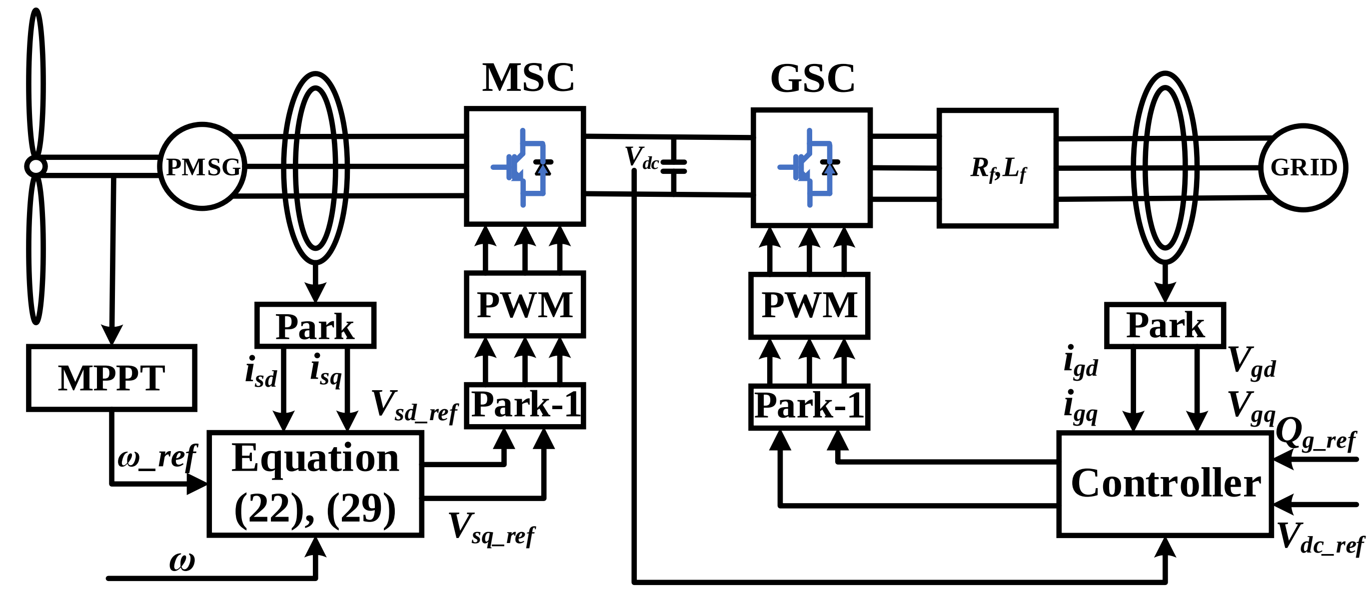

Figure 5. Block diagram of control system in WECS

4. RESULTS

To evaluate the operation of WECS under different wind conditions and test the efficiency of newly designed controllers, the PMSG wind turbine generator system is simulated using MATLAB - Simulink software. Wind speed varies from below rated to above rated according to actual operation situation. The power of the direct drive generator is 1 MW.

Assume a scenario where the wind speed changes in sequence: 5 - 8 - 6 - 12 m/s and the transition time between speeds is 1s as shown in *figure 6* to evaluate the response of the system when the speed wind changes. The performance simulation results of wind turbines and PMSG generators are shown in *figures 7* to 15.

Simulation parameters: Power generator 1 MW, stator resistance 6.25e-3 Ω, generator rotor flux 11.1464 Wb, d axis inductance and q axis inductance 4.229e−3 H, number of pole pairs 75.

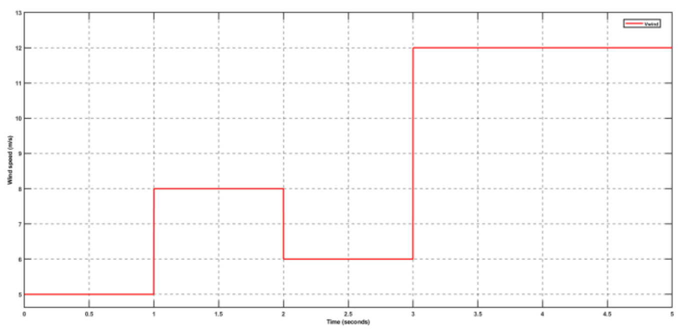

Figure 6. Wind speed

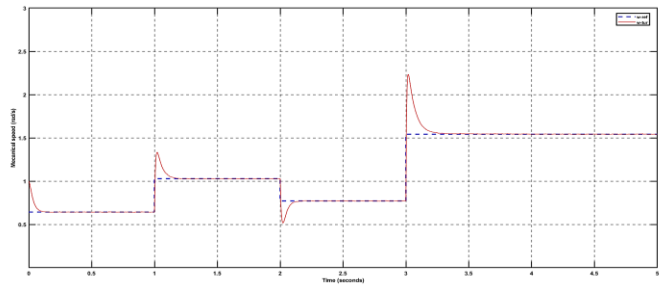

Figure 7. Turbine speed

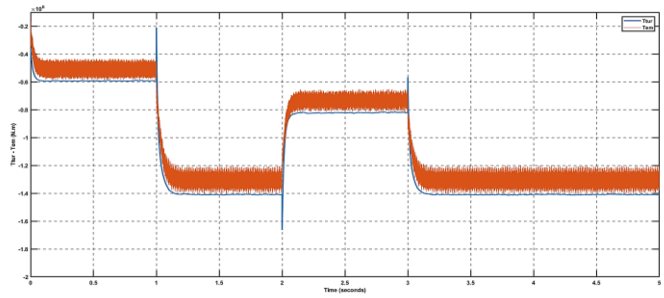

Figure 8. Electromagnetic and mechanical torque

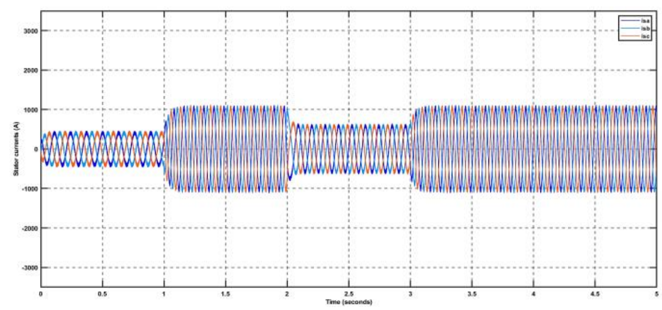

Figure 9. Stator current

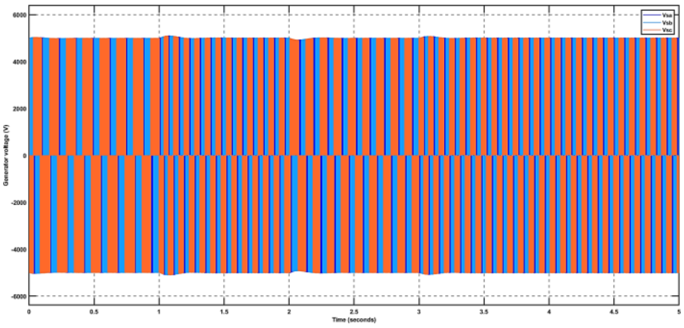

Figure 10. Generator voltage

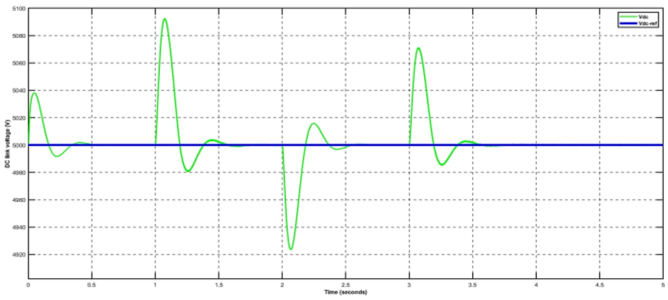

Figure 11. DC link voltage

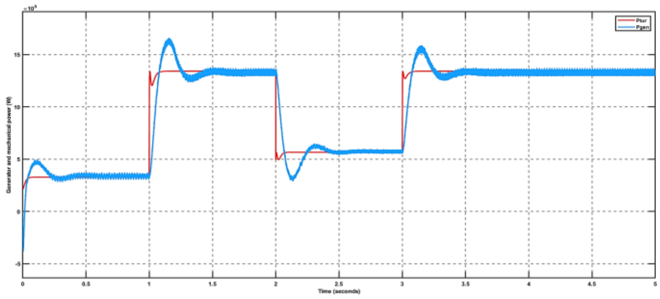

Figure 12. Generator power and mechanical power

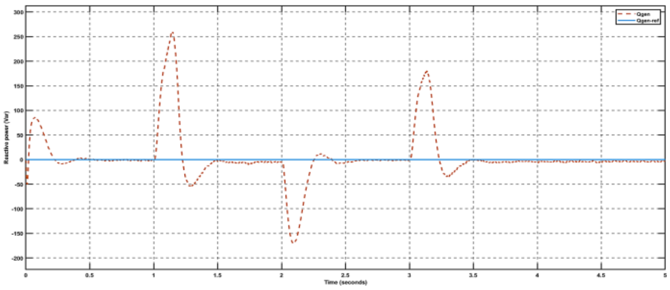

Figure 13. Reactive power

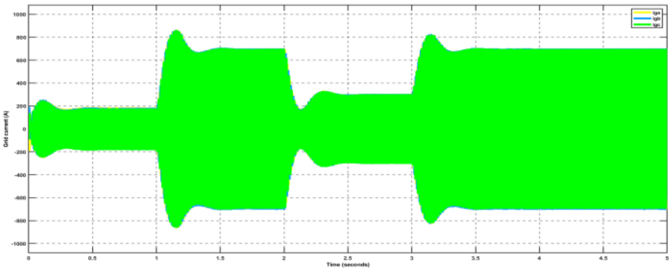

Figure 14. Grid current

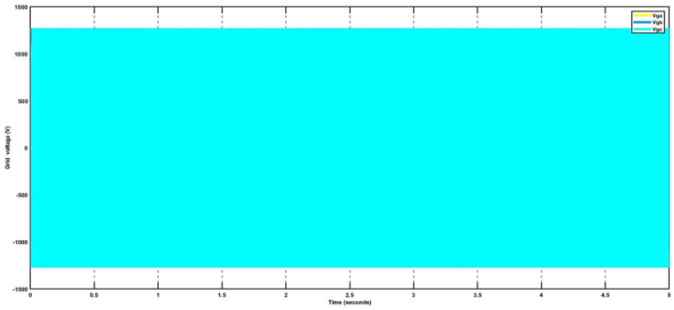

Figure 15. Grid voltage

From the simulation results, we can see that the speed of the wind turbine has tracked the reference value as shown in *figure 7*. The electromagnetic torque is shown in *figure 8*, the smaller the wind speed, the larger the torque, and vice versa, the higher the wind speed, the smaller the torque. *Figure 9* shows that the stator current varies according to the sinusoidal law corresponding to the wind speed change. The voltage of the generator changes according to the sine law with a constant amplitude of 5000V shown in *Figure 10*. The DC bus voltage value of 5000V is always equal to the reference value during operation and is supplied to the unit the GSC side control is shown in *figure 11*. Similarly, the output power is stable and equal to the reference power *figure 12*, reactive power Q is kept zero during operation *figure 13*. The operation of the grid-side converter is shown as shown in Figure 14, *figure 15*. *Figure 14* shows that the grid-side current in the d-q reference frame has i_gq that changes correspondingly to the active power generated on the grid, this value follows reference current. *Figure 15* shows that the quality of voltage supplied to the grid is stable to ensure safety and longevity for the equipment.

The following comparison table shows that the Backstepping control method for the WECS system has many outstanding advantages and is an effective alternative to traditional control methods. Thanks to the ability to operate at various wind speeds, voltage stability is improved and thus helps wind power plants maintain operation, ensuring continuous grid connection for high performance.

Table 1. Performance comparison

Compare methods	Rise time (s)	Settling time (s)	Overshot (%)	Power factor	Performance
Research [40]	0.3	0.4	3.6	0.993	Moderate-high
Proposed method	0.2	0.25	3	0.997	High

5. CONCLUSIONS

This paper has designed current controllers, power controllers and DC link voltage controllers for AC-DC-AC converters. In order to check the operation of the PMSG wind turbine generator system, the simulation results on Matlab - Simulink software are performed in case the wind speed changes corresponding to the actual operating conditions. Simulation results have shown that the control system of the PMSG wind turbine generator works well and stably in the condition of wind speed change. The response of the DC link current, voltage and power always keep track of their reference values. This proves the efficiency of the designed PMSG wind turbine generator control system.

Acknowledgments: The authors gratefully acknowledge the University of Economics – Technology for Industries for supporting this work.

Conflicts of Interest: The author declares no conflict of interest.

REFERENCES

[1] Gupta, R. A., Singh, B., & Jain, B. B. (2015). Wind energy conversion system using PMSG. 2015 International Conference on Recent Developments in Control, Automation and Power Engineering (RDCAPE). doi:10.1109/rdcape.2015.7281395.

[2] Rolan, A., Luna, A., Vazquez, G., Aguilar, D., & Azevedo, G. (2009). Modeling of a variable speed wind turbine with a Permanent Magnet Synchronous Generator. 2009 IEEE International Symposium on Industrial Electronics. doi:10.1109/isie.2009.5218120.

[3] Sharma, H. K., Samaria, A., & Gidwani, L. (2017). Designing and performance analysis of controller for PMSG based wind energy conversion system. 2017 International Conference on Information, Communication, Instrumentation and Control (ICICIC). doi:10.1109/icomicon.2017.8279159.

[4] Kang, L., Shi, L., Ni, Y., Yao, L., & Masoud, B. (2011). Small signal stability analysis with penetration of grid-connected wind farm of PMSG type. 2011 International Conference on Advanced Power System Automation and Protection. doi:10.1109/apap.2011.6180400.

[5] Chi, Y., Liu, C., Tian, X., Shi, L., & Tang, H. (2017). Modeling of Full-scale Converter Wind Turbine Generator. Modeling and Modern Control of Wind Power, 85–115. doi:10.1002/9781119236382.ch5.

[6] Bonfiglio, A., Delfino, F., Gonzalez-Longatt, F., & Procopio, R. (2017). Steady-state assessments of PMSGs in wind generating units. International Journal of Electrical Power & Energy Systems, 90, 87–93. doi:10.1016/j.ijepes.2017.02.002.

[7] Kumar Sharma, H., Samaria, A., & Gidwani, L. (2018). Power Optimization Technique for Small Wind Turbine System Using an Incremental Current Control. 2018 Internat2018 International Conference on Computation of Power, Energy, Information and Communication (ICCPEIC)ional Conference on Computation of Power, Energy, Information and Communication (ICCPEIC). doi:10.1109/iccpeic.2018.8525227.

[8] Baran, J., & Jąderko, A. (2020). An MPPT Control of a PMSG-Based WECS with Disturbance Compensation and Wind Speed Estimation. Energies, 13(23), 6344. doi:10.3390/en13236344.

[9] Nazir, M. S., Mahdi, A. J., Bilal, M., Sohail, H. M., Ali, N., & Iqbal, H. M. N. (2019). Environmental impact and pollution-related challenges of renewable wind energy paradigm – A review. Science of The Total Environment. doi:10.1016/j.scitotenv.2019.05.274.

[10] Olabi, A. G., Wilberforce, T., Elsaid, K., Salameh, T., Sayed, E. T., Husain, K. S., & Abdelkareem, M. A. (2021). Selection Guidelines for Wind Energy Technologies. Energies, 14(11), 3244. doi:10.3390/en14113244.

[11] Nazir, M. S., Ali, N., Bilal, M., & Iqbal, H. M. N. (2020). Potential environmental impacts of wind energy development – A global perspective. Current Opinion in Environmental Science & Health. doi:10.1016/j.coesh.2020.01.002.

[12] Cao, W., Xie, Y., & T, Z. (2012). Wind Turbine Generator Technologies. Advances in Wind Power. doi:10.5772/51780.

[13] Willenberg, D., Winkens, A., & Linnartz, P. (2020). Impact of wind turbine generator technologies and frequency controls on the stable operation of medium voltage islanded microgrids. Electric Power Systems Research, 189, 106760. doi:10.1016/j.epsr.2020.106760.

[14] Apata, O., & Oyedokun, D. T. O. (2017). Wind turbine generators: Conventional and emerging technologies. 2017 IEEE PES PowerAfrica. doi:10.1109/powerafrica.2017.7991295.

[15] Kesraoui, M., Korichi, N., & Belkadi, A. (2011). Maximum power point tracker of wind energy conversion system. Renewable Energy, 36(10), 2655–2662. doi:10.1016/j.renene.2010.04.028.

[16] Heydari, M., & Smedley, K. (2015). Comparison of maximum power point tracking methods for medium to high power wind energy systems. 2015 20th Conference on Electrical Power Distribution Networks Conference (EPDC). doi:10.1109/epdc.2015.7330493.

[17] Zebraoui, O., & Bouzi, M. (2018). Comparative study of different MPPT methods for wind energy conversion system. IOP Conference Series: Earth and Environmental Science, 161, 012023. doi:10.1088/1755-1315/161/1/012023.

[18] Mousa, H. H. H., Youssef, A.-R., & Mohamed, E. E. M. (2021). State of the art perturb and observe MPPT algorithms-based wind energy conversion systems: A technology review. International Journal of Electrical Power & Energy Systems, 126, 106598. doi:10.1016/j.ijepes.2020.106598.

[19] Mohan, M., & Vittal, K. P. (2018). Modeling and Simulation of PMSG-Based Wind Power Generation System. 2018 3rd IEEE International Conference on Recent Trends in Electronics, Information & Communication Technology (RTEICT). doi:10.1109/rteict42901.2018.9012.

[20] Pindoriya, R. M., Usman, A., Rajpurohit, B. S., & Srivastava, K. N. (2017). PMSG based wind energy generation system: Energy maximization and its control. 2017 7th International Conference on Power Systems (ICPS). doi:10.1109/icpes.2017.8387323.

[21] Kim, Y.-S., Chung, I.-Y., & Moon, S.-I. (2015). Tuning of the PI Controller Parameters of a PMSG Wind Turbine to Improve Control Performance under Various Wind Speeds. Energies, 8(2), 1406–1425. doi:10.3390/en8021406.

[22] Frikh, M. L., Soltani, F., Bensiali, N., Boutasseta, N., & Fergani, N. (2021). Fractional order PID controller design for wind turbine systems using analytical and computational tuning approaches. Computers & Electrical Engineering, 95, 107410. doi:10.1016/j.compeleceng.2021.10.

[23] Eltamaly, A. M., & Farh, H. M. (2013). Maximum power extraction from wind energy system based on fuzzy logic control. Electric Power Systems Research, 97, 144–150. doi:10.1016/j.epsr.2013.01.001.

[24] Minh, H. Q., Frédéric, N., Najib, E., & Abdelaziz, H. (2012). Fuzzy Control of Variable Speed Wind Turbine Using Permanent Magnet Synchronous Machine for Stand-Alone System. Smart Innovation, Systems and Technologies, 31–44. doi:10.1007/978-3-642-27509-8_3.

[25] Soliman, M. A., Hasanien, H., Azazi, H. Z., El-kholy, E. E., & Mahmoud, S. A. (2018). An Adaptive Fuzzy Logic Control Strategy for Performance Enhancement of a Grid-Connected PMSG-Based Wind Turbine. IEEE Transactions on Industrial Informatics, 1–1. doi:10.1109/tii.2018.2875922.

[26] Beltran, B., Ahmed-Ali, T., & El Hachemi Benbouzid, M. (2008). Sliding Mode Power Control of Variable-Speed Wind Energy Conversion Systems. IEEE Transactions on Energy Conversion, 23(2), 551–558. doi:10.1109/tec.2007.914163.

[27] Krim, Y., Abbes, D., Krim, S., & Mimouni, M. F. (2017). Classical vector, first-order sliding-mode and high-order sliding-mode control for a grid-connected variable-speed wind energy conversion system: A comparative study. Wind Engineering, 42(1), 16–37. doi:10.1177/0309524x17723202.

[28] Lee, S.-W., & Chun, K.-H. (2019). Adaptive Sliding Mode Control for PMSG Wind Turbine Systems. Energies, 12(4), 595. doi:10.3390/en12040595.

[29] Fathabadi, H. (2018). Optimal control of a wind energy conversion system and a wind turbine. Optimal Control Applications and Methods, 39(4), 1354–1370. doi:10.1002/oca.2415.

[30] Bratcu, A. I., Munteanu, I., & Ceanga, E. (2008). Optimal control of wind energy conversion systems: From energy optimization to multi-purpose criteria - A short survey. 2008 16th Mediterranean Conference on Control and Automation. doi:10.1109/med.2008.4602183.

[31] GAO, X., WANG, X., & HE, J. (2020). Optimal control of pitch angle of large wind turbine based on speed differential. E3S Web of Conferences, 194, 03008. doi:10.1051/e3sconf/202019403008.

[32] Wei, C., Zhang, Z., Qiao, W., & Qu, L. (2015). Reinforcement-Learning-Based Intelligent Maximum Power Point Tracking Control for Wind Energy Conversion Systems. IEEE Transactions on Industrial Electronics, 62(10), 6360–6370. doi:10.1109/tie.2015.2420792.

[33] Wei, C., Zhang, Z., Qiao, W., & Qu, L. (2016). An Adaptive Network-Based Reinforcement Learning Method for MPPT Control of PMSG

International Journal of
Electrical and Electronics Research (IJEER)
Research Article | Volume 12, Issue 2 | Pages 520-528 | e-ISSN: 2347-470X

Wind Energy Conversion Systems. IEEE Transactions on Power Electronics, 31(11), 7837–7848. doi:10.1109/tpel.2016.2514370.

[34] Saenz-Aguirre, A., Zulueta, E., Fernandez-Gamiz, U., Lozano, J., & Lopez-Guede, J. (2019). Artificial Neural Network Based Reinforcement Learning for Wind Turbine Yaw Control. Energies, 12(3), 436. doi:10.3390/en12030436.

[35] TOMIN, N., KURBATSKY, V., & GULIYEV, H. (2019). Intelligent Control of a Wind Turbine based on Reinforcement Learning. 2019 16th Conference on Electrical Machines, Drives and Power Systems (ELMA). doi:10.1109/elma.2019.8771645.

[36] Jaramillo-Lopez, F., Kenne, G., & Lamnabhi-Lagarrigue, F. (2016). A novel online training neural network-based algorithm for wind speed estimation and adaptive control of PMSG wind turbine system for maximum power extraction. Renewable Energy, 86, 38–48. doi:10.1016/j.renene.2015.07.071.

[37] Driss, B., Farhat, S., Abdelilah, K., & Rachid, E. M. A. M. (2020). Adaptive control for variable-speed wind generation systems using advanced RBF Neural Network. 2020 1st International Conference on Innovative Research in Applied Science, Engineering and Technology (IRASET). doi:10.1109/iraset48871.2020.9092.

[38] Douanla, R. M., Kenné, G., Pelap, F. B., & Fotso, A. S. (2018). A Modified RBF Neuro-Sliding Mode Control Technique for a Grid Connected PMSG Based Variable Speed Wind Energy Conversion System. Journal of Control Science and Engineering, 2018, 1–19. doi:10.1155/2018/1780634.

[39] Tanvir, A. A., & Merabet, A. (2020). Artificial Neural Network and Kalman Filter for Estimation and Control in Standalone Induction Generator Wind Energy DC Microgrid. Energies, 13(7), 1743. doi:10.3390/en13071743.

[40] Beddar, A., Bouzekri, H., Babes, B., & Afghoul, H. (2016). Experimental enhancement of fuzzy fractional order PI+I controller of grid connected variable speed wind energy conversion system. Energy Conversion and Management, 123, 569–580. doi:10.1016/j.enconman.2016.06.070.